ELSEVIER

Journal of Economic Behavior & Organization
Vol. 62 (2007) 324–347

JOURNAL OF
Economic Behavior
& Organization

www.elsevier.com/locate/econbase

Homoclinic tangles in a Kaldor-like business cycle model

Anna Agliari [a,*], Roberto Dieci [b], Laura Gardini [c]

[a] *Department Scienze Economiche e Sociali, Catholic University, Piacenza, Italy*
[b] *Department Matematica per le Scienze Economiche e Sociali, University of Bologna, Bologna, Italy*
[c] *Department Economia, University of Urbino, Urbino, Italy*

Received 16 November 2004; received in revised form 26 June 2005; accepted 5 July 2005
Available online 4 October 2006

Abstract

In this paper a nonlinear discrete-time business cycle model of Kaldor-type is considered, to illustrate particular global bifurcations which determine the appearance or disappearance of attracting and repelling closed invariant curves. Such bifurcations sequences, which involve homoclinic tangencies and transversal intersection of the stable and unstable manifolds of saddle cycles, may increase the complexity of the basins of attraction of multiple, coexisting attractors. Particularly, for the business cycle model examined here, such dynamic phenomena explain the co-existence of two stable steady states and an attracting closed curve, with an intricate basin structure, for wide ranges of the parameters.

JEL classification: E32; C62; C69

Keywords: Business cycle; Nonlinear discrete dynamical models; Global bifurcations; Homoclinic tangles; Heteroclinic connections

1. Introduction

The economic literature on complex dynamics has mainly focused on chaotic behavior in dynamic systems with a single attractor. The notion of *complexity* in this case refers to the nature of the *asymptotic dynamics* (i.e. the dynamical properties of the motion on a strange attractor),

* Correspondence to: Università Cattolica del Sacro Cuore, Via Emilia Parmense 84, 29100 Piacenza, Italia. Tel.: +39 0523599191; fax: +39 0523599303.
E-mail addresses: anna.agliari@unicatt.it (A. Agliari), rdieci@rimini.unibo.it (R. Dieci), gardini@uniurb.it (L. Gardini).

0167-2681/$ – see front matter © 2006 Elsevier B.V. All rights reserved.
doi:10.1016/j.jebo.2005.07.009

Appendix

In this Appendix we derive the region of invertibility of the map T in the space of parameters (i.e. we determine the combinations of parameters under which the "backward iteration" of (5) is uniquely defined), so that each point of the phase-space has a unique preimage of *rank-1*. Moreover, for those ranges of parameters where the map is noninvertible, we discuss the question of the number and the location of the preimages of a point of the phase space.

The rank-1 preimages of a point (u, v) are the solutions of the system

$$\begin{cases} u = (1-\gamma-\delta)\, x + \arctan y \\ v = -\mu\gamma x + (1-\mu\sigma)\, y + \mu \arctan y \end{cases}$$

where the unknown variables are x and y. Rearranging the two equations we obtain

$$\begin{cases} x = \frac{(1-\sigma\mu)y - v + \mu u}{\mu(1-\delta)} \\ -(1-\delta-\gamma)\frac{1-\sigma\mu}{\mu(1-\delta)} y + \frac{(1-\delta-\gamma)v + \gamma\mu u}{\mu(1-\delta)} = \arctan y \end{cases} .$$

Then the y-coordinate of the rank-1 preimages of the points (u, v) must satisfy the equation

$$q\,(u, v) + my = \arctan y \tag{12}$$

where $q\,(u, v) = \frac{(1-\delta-\gamma)v + \gamma\mu u}{\mu(1-\delta)}$ and $m = (\gamma+\delta-1)\frac{1-\sigma\mu}{\mu(1-\delta)}$.

Simple geometrical considerations allow us to check that if $m < 0$ or $m \geq 1$, equation (12) has a unique solution for any given (u, v). Therefore if

$$(\gamma+\delta-1)\,(1-\sigma\mu) < 0 \quad \text{or} \quad (\gamma+\delta-1)\,\frac{1-\sigma\mu}{\mu\,(1-\delta)} \geq 1$$

the map T is invertible (i.e. it has a unique inverse). If $m = 0$, then a unique solution of (12) exists if $-\pi/2 < q\,(u, v) < \pi/2$; otherwise no solution exists.

In the case $0 < m < 1$, one, two or three solutions of the equation (12) may exist depending on the value of $q = q\,(u, v)$. In particular, for a given m, $0 < m < 1$, two solutions exist if the straight line at the left side of (12) is tangent to the S-shaped curve $f\,(y) = \arctan y$; that is if

$$m = \frac{1}{1+y^2}$$

so that $y = \mp\sqrt{\frac{1}{m} - 1}$, and

$$\begin{aligned} q\,(u, v) &= q_1 = m\sqrt{\frac{1}{m} - 1} - \arctan\sqrt{\frac{1}{m} - 1} \\ q\,(u, v) &= q_2 = -m\sqrt{\frac{1}{m} - 1} + \arctan\sqrt{\frac{1}{m} - 1} \end{aligned}$$

with $q_1 < q_2$.

Moreover, if $q\,(u, v) < q_1$ or $q\,(u, v) > q_2$ the equation (12) has a unique solution (and the point (u, v) has a unique preimage) while if $q_1 < q\,(u, v) < q_2$ three solutions exist (and therefore three different preimages of the point (u, v)).

This means that if

$$\begin{cases} (1-\delta-\gamma)\,(1-\sigma\mu) < 0 \\ (1-\delta-\gamma)\frac{1-\sigma\mu}{\mu(1-\delta)} > -1 \end{cases} , \tag{13}$$

the map T is noninvertible and, following the notation used in Mira *et al.*, it is a so-called $Z_1 - Z_3 - Z_1$ *map*. With such a notation we indicate that the phase plane is divided in different regions Z_1 and Z_3, whose points have one and three different rank-1 preimages, respectively. Such regions, or *zones*, are separated by the *critical line* LC (i.e. the locus of points having two merging rank-1 preimages).

It follows from the above considerations that the critical line LC is the locus of the points (x, y) of the phase-plane which satisfies[1]

$$q(x, y) = q_1 \quad \text{or} \quad q(x, y) = q_2,$$

and therefore LC is made up by two distinct branches; that is $LC = L^a \cup L^b$ with

$$\begin{aligned} L^a \quad &: \quad x = \frac{(\delta + \gamma - 1)}{\gamma\mu} y + \frac{(1 - \delta)}{\gamma} q_1 \quad \text{and} \\ L^b \quad &: \quad x = \frac{(\delta + \gamma - 1)}{\gamma\mu} y + \frac{(1 - \delta)}{\gamma} q_2 \ . \end{aligned} \tag{14}$$

The locus of the merging preimages of the points belonging to the set LC is the rank-0 critical line LC_{-1} and it is given by $L^a_{-1} \cup L^b_{-1}$, where

$$\begin{aligned} L^a_{-1} \quad &: \quad y = -\sqrt{\frac{1}{m} - 1} \\ L^b_{-1} \quad &: \quad y = \sqrt{\frac{1}{m} - 1} \end{aligned} \tag{15}$$

(i.e. the points which satisfy the tangency condition).

From the noninvertibility conditions (13) we obtain that, for $\delta + \gamma < 1$, the noninvertibility region is an unbounded subset of the (μ, σ)-plane defined by

$$\sigma > \frac{1}{\mu}$$

given that the second condition of (13) is always fulfilled for $0 < \sigma < 1$; for $\delta + \gamma > 1$, the noninvertibility region is defined by

$$\frac{1}{\mu} - \frac{1 - \delta}{\gamma + \delta - 1} < \sigma < \frac{1}{\mu} \ .$$

[1] We recall that the critical line of the map T in (5) may also be obtained by $LC = T\,(LC_{-1})$, where LC_{-1} is the locus of points at which the determinant of the Jacobian matrix vanishes, given in the following equation (15).

and in particular to the unpredictability of the time path of the system in the long-run due to the sensitivity to initial condition. Our knowledge of chaotic behavior of economic systems has largely increased since the introduction of *homoclinic bifurcation theory* into economics: in particular, among other examples, computer assisted proofs of the existence of homoclinic orbits and of the associated complicated dynamic phenomena have been provided by de Vilder (1996) in a two-dimensional OLG model with a Leontief production technology, by Pintus et al. (2000) in a model of a OLG economy with a CES production technology; by Brock and Hommes (1997) in a cobweb model with rational versus naive expectations and nonlinear demand and supply (see also Foroni and Gardini, 2003), and by Droste et al. (2002) in an evolutionary game theoretic model with Cournot competition. These papers have stressed *the importance of homoclinic tangencies and homoclinic tangles of saddles as a source of increasing complexity of the attractors*, which determines the transition from local regular to global irregular fluctuations.

A different source of complicated dynamics, which has received relatively little attention in the economic literature, is associated with the coexistence of attractors. Indeed, when several competing attractors coexist in the phase-space, the structure of their *basins of attraction*, and the dependence of the basin boundaries to the parameters of the model, plays a fundamental role in the long-run behavior. Such situations of coexistence of attractors have been reported for a wide range of nonlinear dynamic economic models in discrete time (see, among others, Brock and Hommes, 1997; Lorenz, 1992; Agliari et al., 2005b; Bischi and Kopel, 2001; Bischi et al., 2003; Puu and Sushko, 2002), and we know that in the case of nonlinear systems the basin boundaries may be quite complex, even in the presence of attractors characterized by a simple structure (e.g., McDonald et al., 1985). A question which arises quite naturally in the case of dynamical systems with multiple attractors is about the nature of the phase-space transitions which lead to the appearance of new attractors or to the disappearance of existing ones (or the related question of the appearance/disappearance of invariant repelling sets) and about the resulting qualitative changes of the structure of the basins. In general these mechanisms consist in sequences of *global*[1] bifurcations. Among them, the bifurcations involved in the appearance, or disappearance, of attracting or repelling *invariant* curves are particularly important, given the attention paid by the economic literature to those mechanisms which lead to the onset of endogenous, long-run fluctuations in economic systems. As we shall see, the typical mechanisms which determine the transition between different situations of coexisting attractors (as well as the qualitative changes of the basins of attraction) are associated once more with *homoclinic bifurcations*.

New results in this direction can be found in Agliari et al. (2005a, 2005b), where particular bifurcation sequences are described which involve attracting and repelling closed invariant curves, characterized by the creation of *heteroclinic* and *homoclinic connections* or *homoclinic tangles*: as shown by means of qualitative phase diagrams, the bifurcation sequences analyzed in such papers are likely to be quite general ones, given that similar sequences must necessarily occur every time a two-dimensional map has a fixed point which may lose stability via a subcritical Neimark-Sacker bifurcation (in Agliari et al., 2005b) or via a supercritical Neimark-Sacker bifurcation and a supercritical pitchfork or flip bifurcation (in Agliari et al., 2005a). Economic examples of the latter kind of maps can be found, for instance, among Kaldorian discrete-time models (see, e.g., Bischi et al., 2001; Agliari and Dieci, 2005). This is the reason why a particular Kaldor-type business cycle model, already proposed and studied in Bischi et al. (2001), will be used in this paper as

[1] These are bifurcations that are not associated with the behavior of the linearization of the dynamical system around its steady states or cycles.

a vehicle to demonstrate the mechanisms underlying the sudden appearance/disappearance of closed invariant curves and the resulting situations of multistability and complexity of the basins. The detection and detailed analysis of such phenomena within a simple and well-known business cycle model may be much more appealing and convincing, for the applied dynamicist, than a more theoretical exposition, such as the one provided in Agliari et al. (2005a). As expected, also in this economic example such dynamic phenomena are related to homoclinic tangles of a saddle point or a saddle cycle, as conjectured in Agliari et al. (2005a).

Though the Kaldor business-cycle model is rather dated and has been criticized on a number of grounds, the simple two-dimensional discrete-time version considered in the present paper will give us the opportunity to highlight further *the role played by heteroclinic and homoclinic connections and homoclinic tangles in the creation of multiple attractors and transition to complex basin structures*. The numerical and graphical analysis which we will carry out on the discrete-time Kaldor model should be considered as a "worked-out example" to guide the mathematical economists to cope with endogenous oscillations, multiple attractors and complex basins, created via global bifurcations in a generic discrete-time model. In other words, we would like to address the question of multi-stability and complexity of the basins via homoclinic tangles in discrete-time economic models, in the same way that the already mentioned literature focuses on the transition to complex asymptotic dynamics (*complexity of the attractors*) via homoclinic bifurcations. This strengthens, in our opinion, the importance of homoclinic bifurcations as a tool of global dynamic analysis of discrete-time economic models.

The paper is organized as follow. In Section 2 we introduce the particular Kaldor-like model studied in Bischi et al. (2001) and discuss the local stability conditions of its equilibria, as well as some properties of the associated map. In Section 3, starting from the situation in which two fixed points exist, we will study the emergence of endogenous fluctuations. We will see that an attracting closed curve appears when the two fixed points are still stable, so that for particular parameter ranges three different kinds of long run behavior exist, depending on the initial condition. We will provide an explanation of the bifurcation sequences which lead to this situation of *multi-stability*, and to the qualitative changes of the basins of attraction of the coexisting attractors. In particular, Section 4 is devoted to exploring a parameter regime where endogenous fluctuations on an attracting closed curve arise via a bifurcation sequence associated with a cycle of period 18 and to explaining the appearance of a repelling set which bounds the set of initial conditions converging to the two fixed points as well as the splitting up of this repelling set into two new repelling closed curves. Section 5 concludes.

2. The model

The model proposed by Kaldor[2] (1940) is one of the earliest and simplest nonlinear models of business cycles. This model was criticized because of its lack of microfoundation, and today it appears very simple and rather dated if compared with the modern approaches to the business cycle. However, since the reformulation of the Kaldor model as a continuous time dynamical system proposed by Chang and Smyth (1971), this model has been generating a considerable amount of economic, pedagogical and methodological interest, both in its continuous-time and discrete-time versions (see, e.g., Varian, 1979; Dana and Malgrange, 1984; Herrmann, 1985; Gabisch and Lorenz, 1989; Lorenz, 1987, 1992, 1993; Grasman and Wentzel, 1994; Dohtani et al., 1996; Bischi et al., 2001).

[2] He himself never studied it as a formal dynamical system.

As it is well known, in the Kaldor business cycle model it is assumed that the global supply Y by firms has as its immediate counterpart an equal amount of income and generates a consumption demand C and an investment demand I, which both depend only on the output Y and the capital stock K. It is also assumed that firms adjust supply Y to demand $C+I$ through a variation of production proportional to excess demand. These assumptions may be formalized through the following well-known discrete-time scheme

$$Y_{t+1} = Y_t + \mu(C_t + I_t - Y_t) = Y_t + \mu(I_t - S_t); \quad K_{t+1} = (1-\delta)K_t + I_t \tag{1}$$

where $S = Y - C$ represents the savings function, $\mu > 0$ is the parameter for the speed of adjustment of supply to demand, δ $(0 < \delta < 1)$ is the rate of depreciation of the capital. Kaldor (1940, 1971) assumed that, for a given K, the total marginal propensity to spend $(\partial C/\partial Y + \partial I/\partial Y)$ is greater than one for "normal" levels of production and less than one for high or low levels of production. A possible way to incorporate this idea into the general model (1) is to use, for instance, a savings function $S = Y - C$ proportional to income ($S = \sigma Y$, where $\sigma = 1 - \partial C/\partial Y$ is the constant propensity to save) and to assume that investment demand is an S-shaped function of income for any given level of capital. Moreover, in Kaldor's original idea the investment and savings schedules are short period functions and are assumed to shift as capital stock shifts: in particular, a rise (fall) in capital stock will shift the investment function down (up). The latter feature can be formalized by assuming that the investment demand is a decreasing function of K, for any given Y. A simple mathematical formulation which satisfies the above requirements is the one proposed in Rodano (1997) and Bischi et al. (2001), in which the saving and investment schedules are specified, respectively, as

$$S_t = \sigma Y_t \tag{2}$$

$$I_t = \sigma\alpha + \gamma\left(\frac{\sigma\alpha}{\delta} - K_t\right) + \arctan(Y_t - \alpha) \tag{3}$$

where the coefficient $\sigma \equiv 1 - \partial C/\partial Y$, $0 < \sigma < 1$, represents the (constant) *propensity to save,* α represents the "normal" level of income (exogenously assumed in firms' expectations), while $\sigma\alpha/\delta$ is the "normal" level of capital stock. In particular, in the investment demand I_t two short run components are considered: the first one is proportional to the difference between normal capital stock and current stock, according to a coefficient γ $(\gamma > 0)$, which captures the presence of adjustment costs; the second one is an increasing S-shaped function of the difference between current income and its "normal" level.

By substituting the expressions of I_t and S_t into the dynamic model (1), we obtain the following two-dimensional nonlinear discrete-time dynamic system:

$$M: \begin{cases} Y_{t+1} = Y_t + \mu[\sigma\alpha + \gamma\left(\dfrac{\sigma\alpha}{\delta} - K_t\right) + \arctan(Y_t - \alpha) - \sigma Y_t] \\ K_{t+1} = (1-\delta)K_t + \sigma\alpha + \gamma\left(\dfrac{\sigma\alpha}{\delta} - K_t\right) + \arctan(Y_t - \alpha) \end{cases}. \tag{4}$$

As it will be stated in the next sections, the dynamical system (4) admits the "exogenous" or "normal" steady state $(\alpha, \sigma\alpha/\delta)$, but it may have further steady states for particular ranges of parameters. A dynamic analysis of the model (4), including local stability analysis of the exogenous steady state and some numerical exploration of the global dynamics, has been performed in Bischi et al. (2001). In that paper, a particular dynamic scenario of multi-stability was discovered for low values of the propensity to save σ and sufficiently high values of the speed of adjustment μ, *where two stable steady states coexist with an attracting invariant closed curve*, and an intuitive

explanation of this phenomenon and of the related basins' bifurcations was provided. The present paper is based upon the same model considered in Bischi et al. (2001), and the focus is again on dynamic scenarios of multi-stability. Nevertheless, the present paper is completely different from Bischi et al. (2001) both in terms of methodological approach, which is largely based on numerical analysis of homoclinic and heteroclinic connections and homoclinic tangles of saddles, and with respect to our level of understanding of the bifurcation mechanisms associated with multistability, which were not explained in detail in Bischi et al. (2001). The interplay between numerical analysis, phase diagrams and results from homoclinic bifurcation theory allows us to understand how such a scenario of multi-stability is created and which bifurcation mechanisms cause the transition to qualitatively different scenarios. Moreover, the thorough numerical analysis of the so-called *homoclinic tangles* (which often take place in very narrow ranges of parameters) allows us to explain the intricate basins' structures which often characterize the transition between different regimes.

2.1. The map and its properties

In order to make as simple as possible the analysis of the model (4), we introduce new coordinates, so that the normal level of income and capital (α, $\sigma\alpha/\delta$) is represented by the origin (0, 0) of the plane; that is, we consider

$$\Phi : \begin{cases} x_t = K_t - \dfrac{\sigma\alpha}{\delta} \\ y_t = Y_t - \alpha \end{cases}.$$

Thus, the model we focus on is

$$T : \begin{cases} x' = (1 - \gamma - \delta)x + \arctan y \\ y' = -\mu\gamma x + (1 - \mu\sigma)y + \mu \arctan y \end{cases}, \tag{5}$$

where the symbol $'$ denotes the unit time advancement operator. Obviously the map T is topologically conjugate to the map M describing the model, and the dynamics of the latter can be obtained from that of (5) by applying the inverse transformation of Φ.

The map T depends on four parameters: the adjustment coefficient γ between normal and current capital stock, the capital stock depreciation rate δ, the speed of adjustment μ and the propensity to save σ; in our analysis we shall consider as parameter space

$$\Omega = \{(\mu, \sigma) : \mu > 0 \text{ and } 0 < \sigma < 1\}$$

fixing the parameters γ ($\gamma > 0$) and δ ($0 < \delta < 1$).

Note that the map T is independent on α; then such a parameter does not affect the asymptotic behavior of the model. It is only a "location" parameter, in the sense that it only indicates the region of the phase plane where the long-run dynamics takes place.

It is simple to observe that the map T is symmetric with respect to the equilibrium point (0, 0), that is, $T(-x, -y) = -T(x, y)$. This means that the generic trajectory generated by the iteration of (5) is either symmetric with respect to the origin or, if not, there exists a symmetric trajectory. This property is important from an economic point of view, since it may give rise to coexistence of attractors; for example, if there exists a cycle of odd period, then the symmetry property implies that there must exist a symmetric cycle of the same period and with the same stability property.

The next sections summarize the main analytical properties (derivation of the steady states, local stability analysis, non-invertibility conditions) of the dynamical system (4), which have already been discussed in Bischi et al. (2001). We repeat here the main analytical results not only for the convenience of the reader (in order to keep the paper self-contained), but also because the discussion is carried out in terms of the map T, which is topologically conjugate to the one studied in Bischi et al. (2001) (and the conditions are here given in terms of the new formulation of the model).

2.2. Local stability analysis

The equilibrium points of the model (5) are the fixed points of T, solutions of the system

$$\begin{cases} x = \dfrac{\sigma}{\delta} y \\ \dfrac{(\gamma+\delta)\sigma}{\delta} y = \arctan y \end{cases} \tag{6}$$

obtained by a trivial manipulation of (5) with $x' = x$ and $y' = y$.

Besides the solution $E^* = (0, 0)$, we can observe that further fixed points exist if the equation

$$\frac{(\gamma+\delta)\sigma}{\delta} y = \arctan y \tag{7}$$

admits non-zero solutions, that is if the straight line of equation $z = ((\gamma+\delta)\sigma/\delta)y$ and the sigmoid-shaped graph of the function $z = \arctan(y)$ intersect in some points other than the origin. Since this occurs if and only if the slope of the straight line is lower than the slope of the function $f(y) = \arctan y$ (at the origin), we can easily state the following.

Proposition 1. *If $\sigma \geq (\delta/(\gamma+\delta))$ then $E^* = (0, 0)$ is the unique fixed point of the map T defined by* (5). *If $\sigma < (\delta/(\gamma+\delta))$ then two further fixed points, P^* and Q^*, exist, symmetric with respect to the fixed point E^*.*

We consider now the conditions of local asymptotic stability of the fixed point $E^* = (0, 0)$, in terms of the parameters of the model. As usual, the stability conditions are derived via the localization, in the complex plane, of the eigenvalues of the Jacobian matrix evaluated at the fixed point (let us denote it by J^*). A well known necessary and sufficient condition for the two eigenvalues of J^* to be smaller than one in modulus (which implies a locally asymptotically stable steady state) is given by the following set of inequalities (see, e.g., Gumowski and Mira, 1980 or Medio and Lines, 2001): $1 - \mathrm{Tr}(J^*) + \mathrm{Det}(J^*) > 0$; $1 + \mathrm{Tr}(J^*) + \mathrm{Det}(J^*) > 0$; $\mathrm{Det}(J^*) < 1$, where $\mathrm{Tr}(J^*)$ and $\mathrm{Det}(J^*)$ denote the trace and the determinant of J^*, respectively. Standard computations (see also Bischi et al., 2001) lead to the following proposition, where obviously we restrict our analysis to $0 < \delta < 1$, $0 < \sigma < 1$, $\alpha > 0$, and we assume in addition $\gamma < 2 - \delta$.[3]

Proposition 2. *The fixed point $E^* = (0, 0)$ is locally asymptotically stable if the parameters μ and σ belong to the region ABCD of the plane (μ,σ), with vertices $A = (0, (\delta/(\delta+\gamma)))$, $B = (0, 1)$, $C = (((\delta+\gamma)/\gamma), 1)$, $D = (((\delta+\gamma)^2/\gamma), (\delta/(\delta+\gamma)))$ where AB belongs to the line $\mu = 0$, BC to the*

[3] The assumed interval of the parameter γ largely includes the range of its economically plausible values.

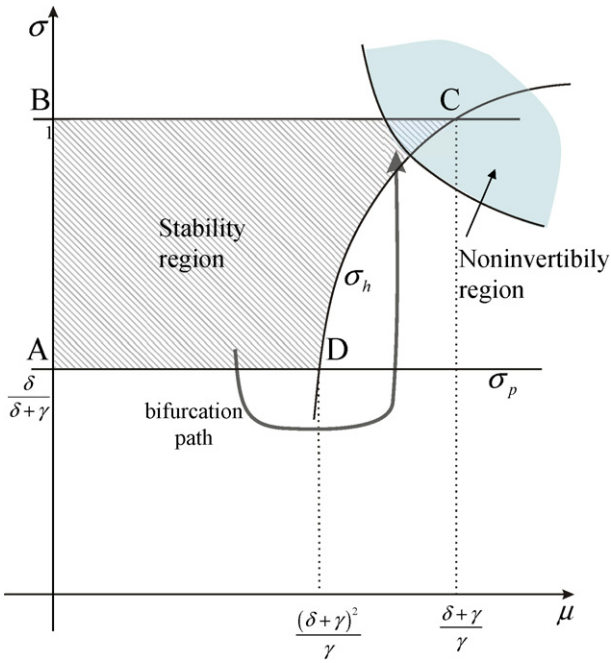

Fig. 1. The stability region of the fixed point E^* and the noninvertibility region of the map T in the case $\gamma < 1 - \delta$.

line $\sigma = 1$ *and the side AD to the line*

$$\sigma = \sigma_{\mathrm{p}} = \frac{\delta}{\delta + \gamma} \tag{8}$$

while the arc connecting C and D belongs to the hyperbola of equation

$$\sigma = \sigma_{\mathrm{h}}(\mu) = \frac{(1-\delta)\mu - \delta - \gamma}{(1-\delta-\gamma)\mu}. \tag{9}$$

Moreover, the arc CD of the stability region represents a Neimark-Sacker bifurcation curve, at which E^* *is transformed from stable to unstable focus, while the segment AD represents a* (*supercritical*) *pitchfork bifurcation boundary, at which* E^* *becomes a saddle and two new stable fixed points appear close to* E^*.

A qualitative draft of the stability region is shown in Fig. 1 in the case $\gamma < 1 - \delta$, which is the one assumed in our numerical simulation.[4]

From Propositions 1 and 2 we deduce that two further equilibria P^* and Q^* emerge when the saving rate is lower than a certain threshold $\sigma_{\mathrm{p}} = \delta/(\gamma + \delta)$, which is directly related to the depreciation rate δ and inversely related to the adjustment coefficient γ. The same quantity also represents the pitchfork bifurcation value of the "normal" stable equilibrium E^*, at which it is transformed into a saddle. The equilibria P^* and Q^* are located in symmetric position with respect to E^*, and the location of the fixed points is independent on the parameter μ. Note that in the limiting case

[4] If $1 - \delta < \gamma < 2 - \delta$ the stability region has the same vertices, but in this case the arc *CD* is negatively sloped. When $\gamma = 1 - \delta$ the side *CD* belongs to the vertical line $\mu = 1/\gamma$.

$\gamma \to 0$, under which the investment (3) turns out to be independent on the capital stock and no "shifting" of the investment curve exists, $\sigma_p \to 1$ and therefore the model admits three steady states for any σ, $0 < \sigma < 1$. In this case no Neimark-Sacker boundary exists and no endogenous fluctuations along a stable closed curve can occur.[5] When a gradual adjustment towards the "normal" level of capital (governed by the parameter $\gamma > 0$) is introduced into the investment function, multiple equilibria are possible provided that the propensity to save is small enough, below the threshold σ_p. When $\sigma < \sigma_p$, *bi-stability* (without oscillations) will be the prevailing dynamic scenario. On the other hand, self-sustaining oscillations emerge for $\sigma > \sigma_p$ when the speed of adjustment μ becomes sufficiently high. Nevertheless, in Section 3 we shall see that also under small values of σ, in the presence of three steady states, long-run oscillatory behavior is possible, provided that μ is high enough. This determines situations of multi-stability. The study of such situations, and of the mechanisms associate with their appearance, is the main topic of this paper.

2.3. Invertibility of the map

For particular constellations of the parameters, the map T defined in (5) is a noninvertible map of the plane. This means that while starting from an initial condition (x_0, y_0) the forward iteration of (5) uniquely defines the trajectory $(x_t, y_t) = T^t(x_0, y_0)$, $t = 1, 2, \ldots$, while the backward iteration of (5) may not be unique. Recent economic literature dealing with cases of multiple attractors in two-dimensional discrete-time dynamical systems represented by noninvertible maps (see, e.g., Bischi and Kopel, 2001, 2003; Foroni et al., 2003; Dieci et al., 2001; Chiarella et al., 2002; Agliari et al., 2000, 2006) has highlighted how noninvertibility can become a source of bifurcations and complex structures of the basins of attraction. However, we must stress that the global phenomena and the complex structures of the basins shown in the present paper are not due to the noninvertibility of the map. Indeed the map is at least locally invertible under the parameter ranges assumed in our numerical simulations. The goal of the present section is therefore to determine the regions of the space of parameters where the map is invertible (and noninvertible), in order to prove that the particular parameter constellation used in our numerical simulation is one where the map is invertible in a sufficiently large region including the attractors. We consider again the (μ, σ)-plane (for fixed values of the remaining parameters) so that the ranges of invertibility or noninvertibility of the map T can be compared with the local bifurcation curves, and we state the following proposition (which is proved in Appendix in Supplementary Material):

Proposition 3. *The (μ, σ)-plane of parameters, $\mu > 0$, $0 < \sigma < 1$, includes a region of noninvertibility of the map* (5). *In particular, in the case $(\delta + \gamma) < 1$, the noninvertibility region is an unbounded set defined by*

$$\sigma > \frac{1}{\mu},$$

while in the case $\delta + \gamma > 1$, the noninvertibility region is defined by

$$\begin{cases} \sigma < \dfrac{1}{\mu} \\ \sigma > \dfrac{1}{\mu} - \dfrac{1-\delta}{\gamma + \delta - 1} \end{cases}.$$

Moreover, in the noninvertibility region the map T is a $Z_1 - Z_3 - Z_1$ map.

[5] This particular case has been considered in detail in Bischi et al. (2001).

The latter statement of Proposition 3, which follows the notation used in Mira et al. (1996), means that the phase plane is divided into different regions Z_1 and Z_3, whose points have one and three different *rank*-1 preimages, respectively. Such regions, or *zones*, are separated by the *critical curve LC* (i.e. the locus of points having two merging *rank*-1 preimages) which in this case is made up of two parallel straight lines in the phase plane, say L^a and L^b, whose equations are provided in Appendix in Supplementary Material. The region Z_3 is the strip of the phase-plane between L^a and L^b.

Here we are interested in the intersection of the noninvertibility region with the region of local stability of E^*. We restrict our analysis to the case $(\delta+\gamma)<1$, which corresponds to more realistic ranges of the parameters. In this case, we immediately deduce from Proposition 2 that the noninvertibility region does intersect the stability region of E^*, since the vertex C belongs to both of them, as shown in Fig. 1. However, when one considers parameter ranges within the noninvertibility region but close to the hyperbola $\sigma=1/\mu$ (as is the case of our simulations), two further preimages of a given point in Z_3 do exist but they are located very far away from the always existing one, so that in a neighborhood of the line $\sigma=1/\mu$ the map can be considered an invertible one, at least locally.

3. Phase space transitions with three coexisting equilibria

As we have seen in Proposition 2, the fixed point E^* can be destabilized either via a pitchfork bifurcation, which leads to the coexistence of three equilibria, or via a Neimark-Sacker bifurcation. Numerical simulations have shown that for a wide range of parameters such a Neimark-Sacker bifurcation is of supercritical type: this means that close to the Neimark-Sacker bifurcation curve, the hyperbola $\sigma=\sigma_h(\mu)$ in (9), an attracting closed curve exists to which the generic trajectory converges. Then, in this case the long-run behavior of the map is periodic (generally of very large period) or quasi-periodic (i.e. endogenous fluctuations are generated).

The results of Proposition 2 come from a linear approximation of the map T, and then they have only a local validity, holding in a neighborhood of the fixed point E^*. A more complete knowledge about the long-run behavior of the map T can be achieved with a global study of the dynamical model. In particular the global analysis allows us to discover further situations of multistability besides the coexistence of two stable steady states and to understand, in particular, whether endogenous fluctuations may emerge also far from the Neimark-Sacker bifurcation curve.

Before proceeding in this study, let us recall some important notions useful to perform the global analysis of the model. Given our two-dimensional example (5), we restrict our presentation to the case of invertible maps defined in R^2, since under our parameter selection the map T is invertible, at least locally. Our references on these topics are Guckenheimer and Holmes (1983), Kuznetsov (2003), Palis and Takens (1994), and Mira et al. to which we address the reader for more details and information.

A set S is an *invariant set* for a map G if and only if $G(S)=S$. The simplest examples of invariant sets are the fixed points and the cycles of the map. More generally, the attracting (repelling) sets and the attractors (repellors) of a map are invariant sets. Strictly speaking, an *attracting set* A is a closed invariant set such that there exists a neighborhood U of A strictly mapped in itself and whose trajectories (i.e. the trajectories starting from all the points of U) converge to A while an *attractor* is an attracting set containing a dense orbit. An invariant set not attracting is a *repelling set*.

As the definition suggests, there exist points which converge to an attracting set (or to an attractor) A: the invariant set made up by these points is *the basin of attraction* of A and it can be obtained by considering the union of the preimages of any rank of the neighborhood U.

Other important invariant sets in the study of the global property of an invertible map G are the stable and unstable sets of an hyperbolic[6] fixed point p^*, which are defined as

$$W^{\mathrm{s}}(p^*) = \left\{ x : \lim_{n\to+\infty} G^n(x) = p^* \right\} \tag{10}$$

$$W^{\mathrm{u}}(p^*) = \left\{ x : \lim_{n\to+\infty} G^{-n}(x) = p^* \right\}, \tag{11}$$

respectively.

If p^* is a stable fixed point, the stable set coincides with its basin of attraction. If p^* is a saddle, $W^{\mathrm{s}}(p^*)$ ($W^{\mathrm{u}}(p^*)$) is a one-dimensional smooth curve passing through p^* and tangent at p^* to the stable (unstable) eigenspace. In the following, we will consider the stable (unstable) set as given by the union of two branches merging in p^* denoted by ω^1 (α^1) and ω^2 (α^2). The same definitions can be given for a cycle of period r, by simply considering the union of the stable (unstable) sets of the points of the cycle obtained from (10) ((11)) with the map G^r instead of G, thus the stable set of the cycle $\mathcal{C} = \{p_1, p_2, \ldots, p_r\}$ is

$$W^s(\mathcal{C}) = \bigcup_{i=1}^{r} W^s(p_i)$$

where

$$W^s(p_i) = \left\{ x : \lim_{n\to+\infty} G^{rn}(x) = p_i \right\}$$

and analogously for the unstable set.

The importance of the stable and unstable sets is related to the fact that they are global concepts, that is, they are not defined only in a neighborhood of the fixed point (or cycle). And, if the map is nonlinear, the stable and unstable sets may intersect, so that there may exist a point q such that

$$q \in W^{\mathrm{s}}(p^*) \cap W^{\mathrm{u}}(p^*).$$

This point q is an *homoclinic point* and it can be proved that if an homoclinic point exists, then infinitely many homoclinic points must exist, accumulating in a neighborhood of p^*. Intuitively, this can be understood by observing that the backward and forward orbits of q converge to p^*. The union of the backward and forward orbits of an homoclinic point q is called *homoclinic orbit*. The existence of homoclinic orbits causes a very complex configuration of W^{s} and W^{u}, called *homoclinic tangle*, due to their winding in proximity of p^*. Usually the existence of a homoclinic tangle is related to a sequence of bifurcations occurring in a certain parameter range: first, a homoclinic tangency between a branch of the stable set of the saddle and a branch of the unstable one, followed by a transverse crossing between the stable and unstable set of the saddle cycle, that gives rise to a homoclinic connection, and by a second homoclinic tangency, which closes the sequence. It is worth recalling that in the parameter range in which the manifolds intersect transversely, a chaotic repellor exists, made up of infinitely many (countable) repelling cycles and uncountable aperiodic trajectories, as stated in the Smale-Birkhoff theorem. This chaotic repellor exists after the first homoclinic tangency and disappears after the second one.

[6] A fixed point p^* is said to be hyperbolic if the eigenvalues of the jacobian matrix evaluated at p^* do not belong to the unit circle.

At the end of the homoclinic tangle (i.e. after the second homoclinic tangency), the dynamic behavior of the two branches involved in the bifurcation is modified, *and therefore we can detect the sequence of bifurcations looking at the behavior of* W^s *and* W^u.

Observe that if the saddle is a cycle $\mathcal{C}$, we may have intersection points between the stable and unstable sets of the same periodic point, still called homoclinic points, but also points belonging to the intersection of the stable and unstable sets of different periodic points: in such a case we will call them *heteroclinic points* and *heteroclinic tangle* the corresponding configuration of W^s and W^u.

Apart from the connection to chaotic dynamics, the homoclinic (heteroclinic) tangles play a fundamental role in the bifurcations involving invariant closed curves, as shown in Agliari et al. (2005a). In fact, in that paper the mechanism causing the appearance/disappearance of closed invariant curves is associated with heteroclinic tangles of some saddle cycle.

Since we are interested in the global properties of the map T in (5), we shall study its invariant sets through a continuous dialogue between analytic, geometric and numerical methods and focus our attention on the basins of attraction of the coexisting attractors and on the stable and unstable sets of some saddle points or cycles.

Let us now return to the study of the dynamics of the map T in (5), looking in particular at the coexistence of attractors and to the appearance of self-sustaining oscillations. We start with a numerical investigation of the long-run behaviors of T, following a bifurcation path, shown in Fig. 1, which connects the pitchfork bifurcation curve (the straight line (8)), and the Neimark-Sacker bifurcation curve (the hyperbola (9)). In doing so, we note that a quite generic (i.e. occurring in a large set of parameter constellations) sequence of bifurcations occurs.

We show such a sequence by fixing $\delta = 0.2$, $\gamma = 0.6$, but the same phenomena could be observed for different parameter sets as well. We know that crossing the line $\sigma = \sigma_p$, the fixed point E^* becomes a saddle point, and two distinct stable fixed points (nodes), P^* and Q^*, appear. Let us call $\mathcal{A}$ the attracting set given by the union of the two fixed points, that is, $\mathcal{A} = \{P^*, Q^*\}$ These points are symmetric with respect to E^*, as well as their basins of attraction which are separated by the stable manifold of E^* (see Fig. 2a).[7]

As the adjustment speed μ is increased, the two nodes turn into stable foci, their basins of attraction still being separated by the stable set of E^*, which shows some convolutions around the equilibria (Fig. 2b).

Such convolutions accumulate more and more as the parameters move towards the hyperbola $\sigma = \sigma_h(\mu)$ in (9), revealing that a global bifurcation is occurring. Indeed, as shown in Fig. 2c obtained by increasing the propensity to save σ, an attracting closed curve Γ_s appears, coexisting with the two stable foci and enclosing them. The *global* effect from the point of view of the basins of attraction is dramatic: now we have the coexistence of three different attractors, the two fixed points and the attracting closed curve Γ_s; the latter now attracts all the trajectories starting from outside. This proves that long-run self-sustaining oscillatory behaviors do exist even at small values of the propensity to save ($\sigma < \sigma_p$), although coexisting with no oscillatory ones. The basin of attraction of Γ_s is separated by that of the attracting set $\mathcal{A}$ by a repelling closed curve Γ_u (see the enlargement of Fig. 2c), which seems to appear at the same time of Γ_s. Note however that at this first stage, where the two curves have just appeared, no changes have occurred yet in the basins of attraction *locally* (i.e. in a neighborhood of E^*). From the point of view of the economic interpretation, this implies that a small exogenous shock which moves the economy away from

[7] More details can be seen on the website, where color figures are available.

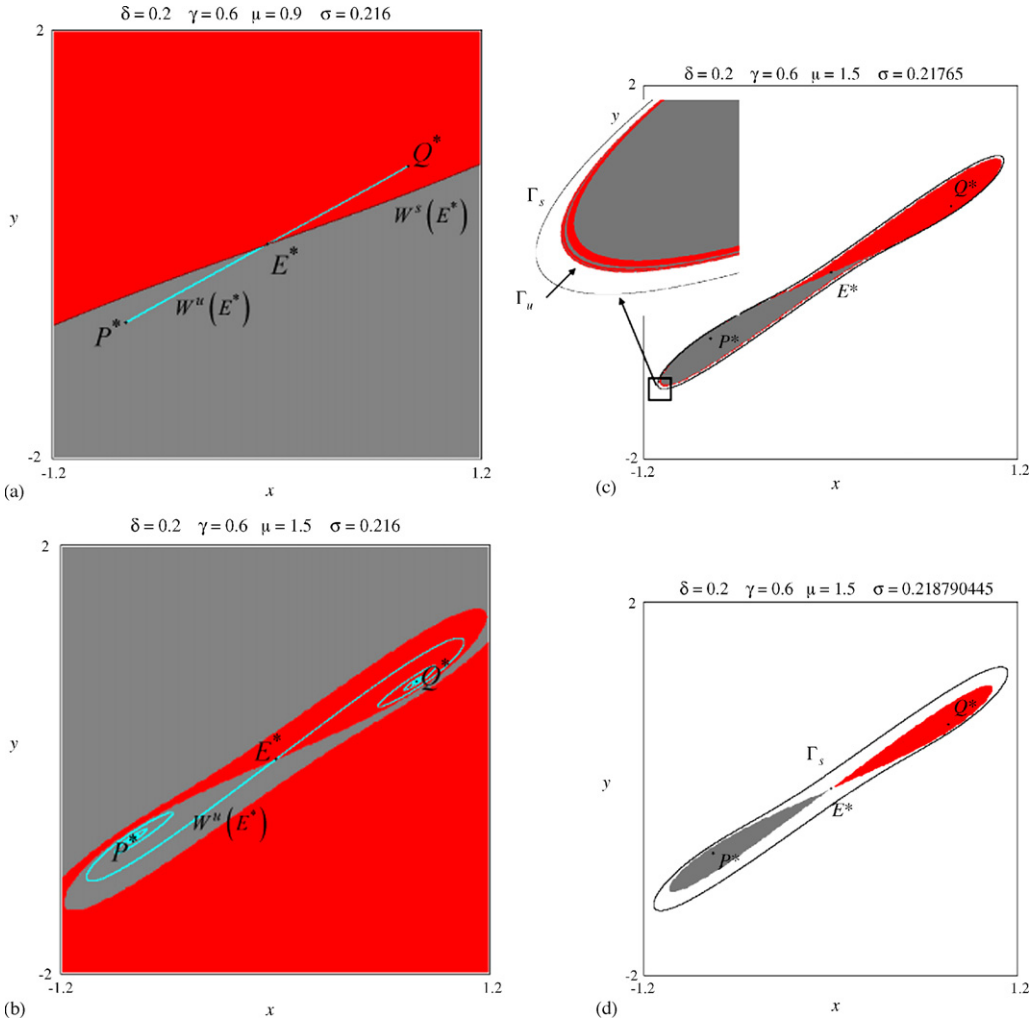

Fig. 2. Coexistence of attractors: (a) two coexisting stable nodes, P^* and Q^*. The basins of attraction of P^* and Q^* (gray and red points, respectively) are separated by the stable set $W^s(E^*)$ of E^*. The unstable set $W^u(E^*)$ (in light blue) converges to the fixed points. (b) The two equilibria have turned into foci and the stable set of E^*, still separating their basins, exhibits same convolutions. (c) The attracting closed curve Γ_s coexists with the two stable foci. Its basin of attraction (white points) is separated from that of the attracting set $\{P^*, Q^*\}$ by a repelling closed curve Γ_u. (d) Γ_u splits in two repelling closed curves which constitute the boundaries of the basins of attraction of P^* and Q^*, respectively. (For interpretation of the references in colour in the figure legends, the reader is referred to the web version of this article.)

the (unstable) normal equilibrium E^* gives rise to a trajectory that eventually settles down in either P^* or Q^*, with the stable set of E^* acting as a "watershed", exactly as it was before the appearance of the curves. Put differently, though a new attracting curve Γ_s now exists, long-run fluctuations are possible only if the economy starts sufficiently far away from the normal steady state E^*.

This dynamic scenario will be analyzed more in details in the next section, with particular attention to the global mechanism causing the appearance of the two invariant curves.

Proceeding further along the bifurcation path, we observe that the repelling closed curve splits in two distinct closed curves, each one bounding the basin of attraction of one of the stable foci,

which gradually reduces in size, as in Fig. 2d. Differently from the previous one, this new global bifurcation does not affect the existing attractors; rather, it produces a qualitative change of the basins of attraction in a neighborhood of E^*, in that a small displacement of the system from E^* now results in oscillatory behavior along the attracting curve Γ_s in the long-run. Notice that this local effect on the basins of attraction could not be detected by looking at the linearized system around the steady states because E^* is still a saddle while P^* and Q^* are still attracting foci. Thus, once more the mechanism underlying the appearance of these two repelling closed curves is related to some global bifurcation and therefore needs a deeper analysis, which will be carried out in Section 4.2.

Approaching again the curve $\sigma = \sigma_p$ in (8) (now from below), the two repelling closed curves shrink on P^* and Q^*, respectively, merging with them at a Neimark-Sacker bifurcation of subcritical type, which leaves two repelling foci and the closed curve Γ_s as unique attractor.

Then the repelling foci turn into repelling nodes and merge with E^* when the bifurcation path crosses again the line (8), but outside the stability region. As a result of such a pitchfork bifurcation, the saddle E^* becomes a repelling node, which turns into a repelling focus encircled by Γ_s. We are approaching the supercritical Neimark-Sacker bifurcation, the hyperbola in (9), after which E^* becomes an attracting focus and the curve Γ_s disappears, merging with E^* itself.

4. Global bifurcations associated with closed invariant curves

In this section we analyze the bifurcation associated with the appearance of the closed invariant curves, anticipated in the previous section. In order to describe the global bifurcations causing the appearance of invariant curves, we follow a vertical bifurcation path, fixing the parameter $\mu = 10$. Indeed, at this value of the speed of adjustment the phenomena previously described are observable in a sufficiently wide range of σ, and thus it will be simpler to follow the mechanisms which cause the appearance of the invariant closed curves. In particular, in this example the attracting closed curve appears as a saddle-focus connection; that is, there exists a periodic orbit, a stable focus cycle of period 18, coexisting with a period 18 saddle cycle, and the unstable manifold of the saddle cycle connects the periodic points of the stable cycle. Then we will be able to study the behaviors of the stable and unstable sets of the saddle cycle and to discover whether any homoclinic or heteroclinic tangle are associated with the appearance of the attracting closed curve.

We recall that (see Section 2.3) at $\mu = 10$ the map is noninvertible if $\sigma > 0.1$, but we will allow the parameter σ to vary in a small neighborhood of 0.1, so that the map is locally invertible in the region of the phase space where the dynamics take place. We start our analysis by increasing σ from $\sigma = 0.09$.

4.1. On the appearance of the attracting closed curve

At $\sigma = 0.09$, P^* and Q^* are attracting foci, with basins of attraction separated by the stable set of the saddle E^*, $W^s(E^*)$, which is a smooth curve coming from the boundary of the basin of attraction of the attracting set $\mathcal{A} = \{P^*, Q^*\}$: the phase space is similar to the case illustrated in Fig. 2b. As the value of σ is increased, $W^s(E^*)$, the curve separating the basins of attraction of the two stable fixed points, presents more and more oscillations in a region quite far from the saddle E^*, as shown in Fig. 3a. This causes an increasing complexity of the boundary separating the basins of attraction of the two stable foci and makes it difficult to forecast the fate of a trajectory starting from the area interested by the winding of $W^s(E^*)$.

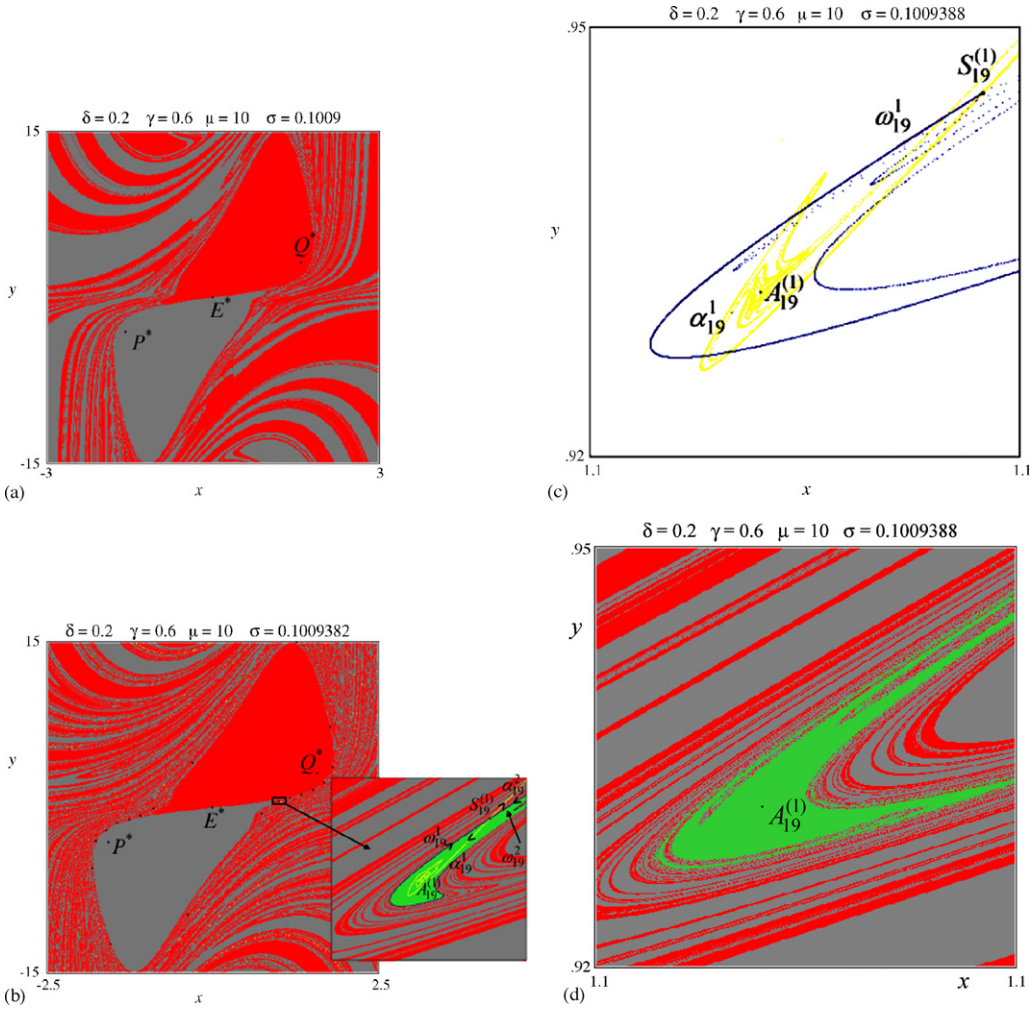

Fig. 3. Appearance of the cycles of period 19. (a) $W^s(E^*)$, separating the basins of attraction of the two stable fixed points, presents more and more convolutions. (b) Two attracting cycles of period 19 exists as well as two saddle cycles of the same period. The basins of attraction of the two stable cycles (green and yellow points) are very narrow and clearly visible in the enlargement. $\mathcal{A}_{19}^{(1)}$ is a periodic point of the cycle $\mathcal{A}_{19}$ of coordinates (1.1547517, 0.9365419). $\mathcal{S}_{19}^{(1)}$ denotes a periodic point of the saddle $\mathcal{S}_{19}$ and $\alpha_{19}^i(\omega_{19}^i)$, $i = 1, 2$, the branches of the unstable (stable) set of $\mathcal{S}_{19}$. (c) Transversal crossing of the stable and unstable sets of the saddle $\mathcal{S}_{19}$, denoting the occurrence of a homoclinic tangle which involves the branches α_{19}^1 and w_{19}^1. (d) The existence of a chaotic repellor due to the homoclinic tangle implies the complex structure of the basins of attraction of the different attractors.

As in the previous section, the particular structure of the stable set of E^* suggests that some bifurcation is incoming. Indeed at $\sigma \sim 0.1009378$ two stable cycles of period 19 appear via saddle-node bifurcation together with two saddle cycles. We illustrate the new situation in Fig. 3b obtained at a slightly higher value of σ, at which the stable node cycles have already turned into foci. At this parameter constellation, after the saddle-node bifurcation, there exist four coexisting attractors: the two fixed points and the two cycles of period 19. The size of the basins of attraction of the two cycles of period 19 is so small that it can only be appreciated in the enlargement of Fig. 3b.

The existence of two pairs of cycles of odd period 19 is due to the symmetry of the map, and in the following we will only refer to one of them, since they have analogous dynamic properties. In the following we will denote the stable focus cycle with $\mathcal{A}_{19}$ and the associated saddle cycle with $\mathcal{S}_{19}$.

The basin of attraction of the cycle $\mathcal{A}_{19}$ is bounded by the stable manifold of the saddle $\mathcal{S}_{19}$, $W^{\mathrm{s}}(\mathcal{S}_{19}) = \omega^1_{19} \cup \omega^2_{19}$ which is a smooth curve surrounding the points of the stable cycle and coming from the boundary of the set of bounded trajectories. The unstable manifold $W^{\mathrm{u}}(\mathcal{S}_{19})$ has a branch (the external one, α^1_{19}) which reaches the points of the stable cycle, turned into a focus, and another branch (the internal one, α^2_{19}) which reaches the two fixed points, crossing the stable set of the saddle E^*. As we can observe from the enlargement of Fig. 3b the branch α^1_{19} shows some oscillations converging to $\mathcal{A}_{19}$ and the branch ω^1_{19} approaches α^1_{19} turning around the periodic points of $\mathcal{A}_{19}$. As the parameter σ is slightly increased, a transversal crossing between the external branch of the unstable set of the saddle $\mathcal{S}_{19}$ and the branch ω^1_{19} of the stable one can be detected (see Fig. 3c). This means that we are inside a *homoclinic tangle* (because the two branches α^1_{19} and ω^1_{19} are related to the same periodic point of the saddle $\mathcal{S}_{19}$). Thus, at a certain value of the parameter a tangential contact between the two branches of the stable and unstable sets has occurred, followed by a transverse intersection in a suitable parameter range. As a consequence, a chaotic repellor has been created, it exists after the first tangential contact and persists during the transverse crossing, and it will disappear after the second tangential contact. This chaotic repellor is responsible of the complex structure of the basins of attraction of the four coexisting attractors: in the enlargement of the phase space shown in Fig. 3d we can see that the basins of attraction of $\mathcal{A}_{19}$ and of the attracting set $\mathcal{A} = \{P^*, Q^*\}$ have a complex structure. Note that some bifurcation similar to the one just described, eventually involving cycles of higher period (attracting or repelling), may also have occurred at smaller values of σ, causing the complex structure of the basins of P^* and Q^* in Fig. 3a.

By increasing the parameter σ, the stable focus $\mathcal{A}_{19}$ turns into a node and it is subject to a sequence of period doubling bifurcations leading to a chaotic attractor: we have followed this route up to a four pieces chaotic attractor of the map T^{19} (that is a 76-piece chaotic attractor of T) which seems to disappear via a final bifurcation, due to a contact with its basin boundary. When this occurs, the stable and unstable sets of $\mathcal{S}_{19}$ always present transverse intersection, which involves also the unstable branch α^2_{19}.

Meanwhile, a new pair of cycles appears via saddle-node: an attracting node of period 18, $\mathcal{A}_{18}$, and the associate saddle, $\mathcal{S}_{18}$. As shown in Fig. 4a, the basin of attraction of the cycle $\mathcal{A}_{18}$, which has turned into a focus, is bounded by the stable set of $\mathcal{S}_{18}$, $W^{\mathrm{s}}(\mathcal{S}_{18}) = \omega^1_{18} \cup \omega^2_{18}$, which comes from the boundary of the set of bounded trajectories. The external branch α^1_{18} of the unstable set converges to $\mathcal{A}_{18}$ and the internal one, α^2_{18}, to the two fixed points, crossing the stable set of the saddle E^*.

Once more, increasing the parameter σ, the internal branch α^2_{18} approaches the branch ω^2_{18}, as shown in Fig. 4b where the basin boundary of $\mathcal{A}_{18}$ is given by the stable set of $\mathcal{S}_{18}$. This means that a heteroclinic tangency has occurred, involving the stable and unstable sets of different periodic points of the saddle cycle $\mathcal{S}_{18}$. The heteroclinic transversal intersection is more evident in Fig. 4c and d, where the tangle develops and the basins of the cycle $\mathcal{A}_{18}$ and of the attracting set $\mathcal{A}$ are intermingled.

Moreover, we recall that the cycles of period 18 coexist with other saddle cycles, the two that appeared via saddle-node bifurcation, $\mathcal{S}_{19}$ and its symmetric one, and those due to the flip bifurcation sequences of the two cycles of period 19, $\mathcal{A}_{19}$ and its symmetric one. Then, different sources of chaotic dynamics are possible in the parameter range we are analyzing. We choose, for

the sake of simplicity, to limit ourself to the study of the saddle cycle $\mathcal{S}_{19}$ and we show in Fig. 4e an enlargement of its unstable set which converges to the focus cycle $\mathcal{A}_{18}$ and to the two fixed points P^* and Q^*. In the same figure is also shown the branch ω^1_{19} of the stable set of $\mathcal{S}_{19}$: we can observe that the transversal crossing with both the branches of the unstable set still persist, but the end of the tangle is coming.

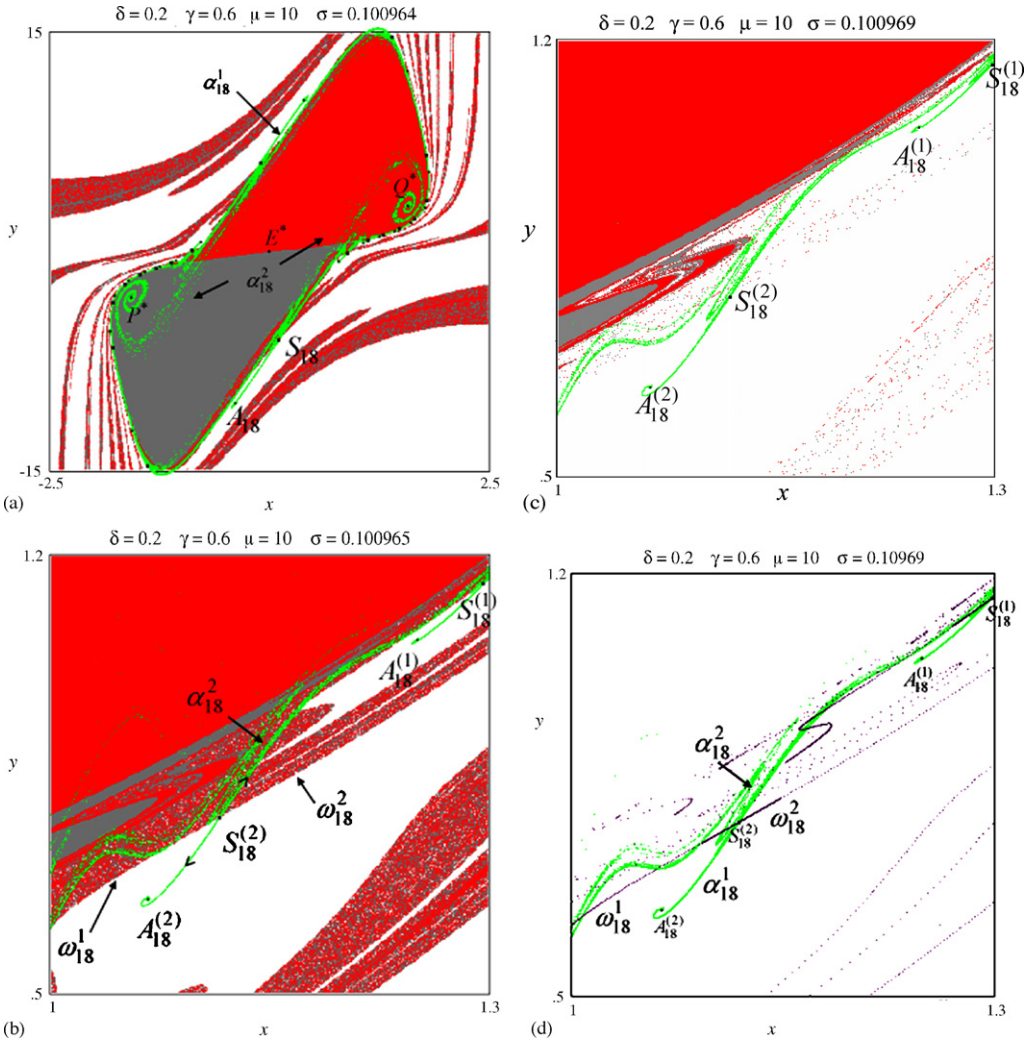

Fig. 4. Appearance of the cycles of period 18. (a) An attracting cycle $\mathcal{A}_{18}$ of period 18 (focus) exists as well as a saddle cycle $\mathcal{S}_{18}$ of the same period. The basin of attraction of $\mathcal{A}_{18}$ is quite large, bounded by the stable set of $\mathcal{S}_{18}$. The branch α^1_{18} of the unstable set of the saddle cycle reaches the periodic points of $\mathcal{A}_{18}$, α^2_{18} reaches the two stable foci P^* and Q^*. (b) An enlargement of the basins of attraction shows the existence of a transversal crossing between the branch α^2_{18} (in green) of the unstable set of the periodic point $\mathcal{S}^{(2)}_{18}$ of $\mathcal{S}_{18}$ and the branch ω^1_{18} of $\mathcal{S}^{(1)}_{18}$. (c) In the homoclinic tangle parameter range, the basins of attraction of $\mathcal{A}_{18}$ and of $\{P^*, Q^*\}$ are intermingled. (d) Transversal crossing between the stable (in violet) and unstable (in green) sets of the saddle $\mathcal{S}_{18}$. (e) Transversal crossing between the stable (in blue) and unstable (in yellow) sets of the saddle $\mathcal{S}_{19}$.

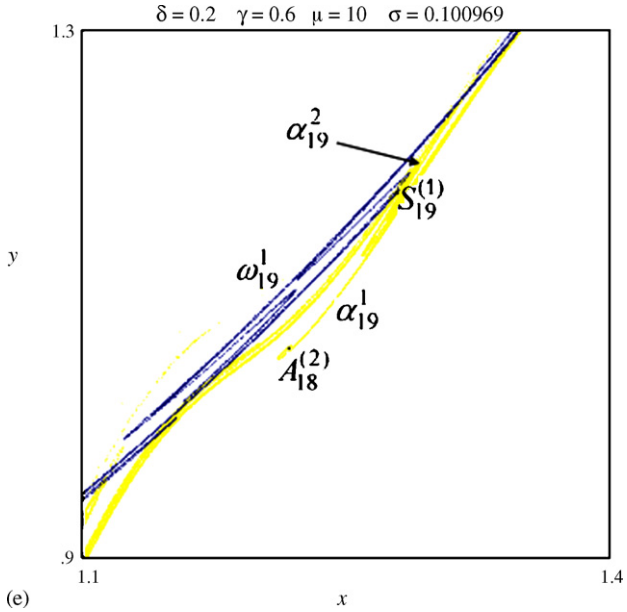

Fig. 4. (*Continued*).

Indeed, at $\sigma = 0.10097$, the two branches α_{19}^1 and α_{19}^2 have no more contacts with ω_{19}^1, as shown in Fig. 5a. At the same parameter values, a repellor, say $\mathcal{F}$, which seems a *weekly chaotic ring* has appeared. The branch ω_{19}^1 of the stable set of the saddle $\mathcal{S}_{19}$ issues from $\mathcal{F}$ as well as the stable manifold of the saddle E^*. This repellor may include the connection of the two saddle cycles (or some other of the existing saddles) with some repelling cycle (cycles) that survived in the tangle. As shown in Fig. 5b, *the repellor $\mathcal{F}$ is the boundary of the basin of attraction of the attracting set $\mathcal{A}$, which now is a bounded set*. $\mathcal{A}$ coexists with the stable focus cycle $\mathcal{A}_{18}$, that now has a wider basin of attraction, to which the unstable set of $\mathcal{S}_{19}$ converges.

The chaotic regime does not end together with the closure of this homoclinic tangle, since the branch α_{18}^2 of the unstable set of $\mathcal{S}_{18}$ is still involved in the homoclinic tangle with the branch ω_{18}^2 of the stable one, as shown in Fig. 5c. This situation cannot be detected simply looking at the basin of attraction of $\mathcal{A}_{18}$ since this heteroclinic tangle only affects the behavior of the map T^{18}. But if we look at the trajectories starting from the area interested by the transverse crossing we observe a quite *long transient* part before the convergence to the focus cycle, which signals the presence of a chaotic repellor.

Moreover, the invariant stable and unstable sets of the saddle $\mathcal{S}_{19}$ have many intersections with those of the saddle $\mathcal{S}_{18}$, and the unstable branch α_{19}^2 has an heteroclinic tangle with ω_{19}^2; these tangles develop until the saddle cycle of period 19 disappears via a saddle-node bifurcation, merging with a stable node of period 19, resulting from a sequence of period halving bifurcations. As a starting attractor, giving rise to such a sequence, we have detected a 76-piece chaotic attractor.

Finally, also the heteroclinic tangle of the saddle $\mathcal{S}_{18}$ arrives at the second tangential contact, after which the chaotic repellor associated to it disappears. In Fig. 5d an enlargement of the stable and unstable sets of $\mathcal{S}_{18}$ is shown. We may observe that the internal branch of $W^{\mathrm{s}}(\mathcal{S}_{18})$ issues from the set $\mathcal{F}$, and the unstable set $W^{\mathrm{u}}(\mathcal{S}_{18})$ gives rise to a closed connection between the periodic points of the stable focus $\mathcal{A}_{18}$, an attracting closed curve now exists, as shown in Fig. 5e.

Summarizing, we have shown that in our example the repelling and attracting closed curves do not appear at the same time. First the repelling set $\mathcal{F}$ (which substitutes the repelling closed curve Γ_s of Fig. 2c) appears at the closure of the homoclinic tangle of the saddle $\mathcal{S}_{19}$, then the attracting closed curve appears at the closure of the heteroclinic tangle of the saddle $\mathcal{S}_{18}$.

Though the phase space representation in Fig. 2c, where the attracting closed curve Γ_s and the repelling closed curve Γ_u look as though they have appeared simultaneously, may

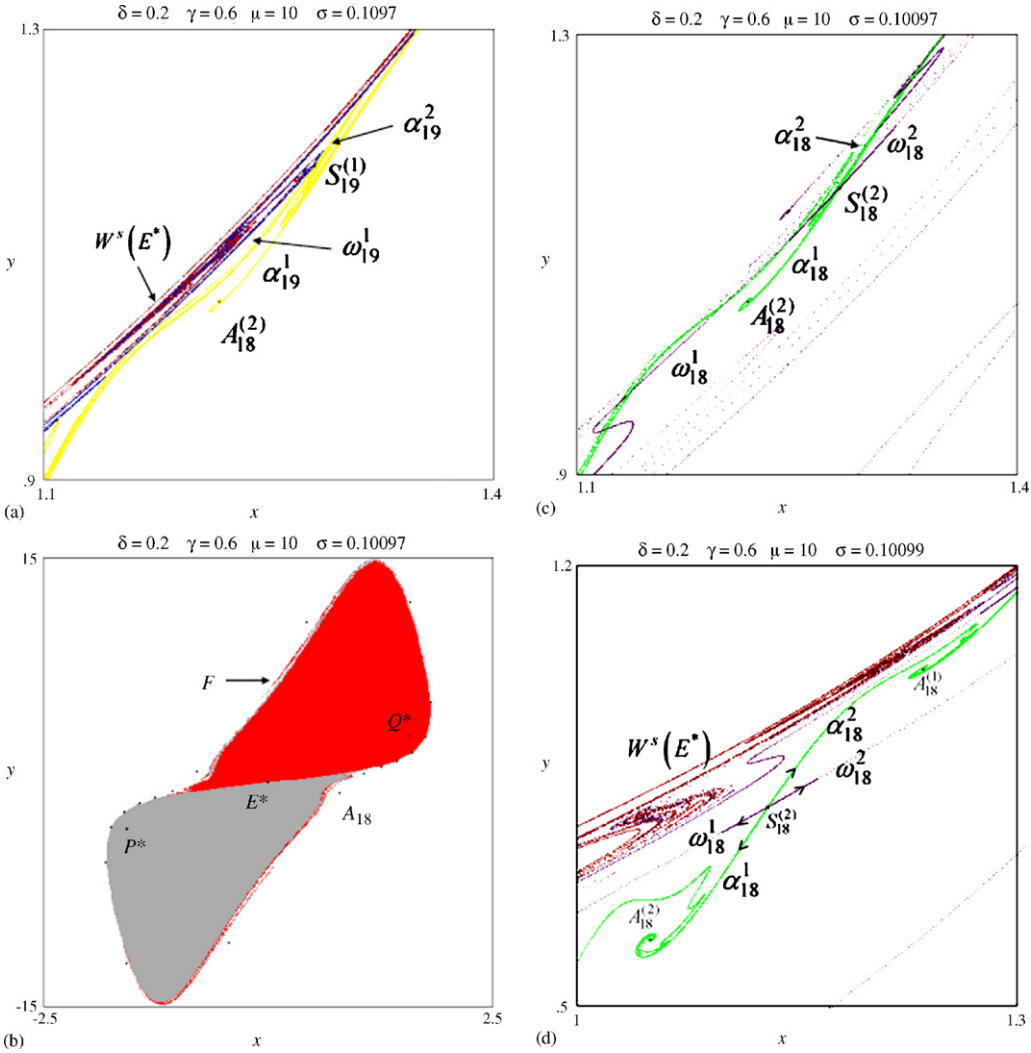

Fig. 5. Closure of the tangles and appearance of closed invariant curves. (a) After the closure of the tangle involving the saddle of period 19, the stable branch ω^1_{19} comes from a strange repellor $\mathcal{F}$ and the unstable branch α^1_{19} converges to the focus cycle $\mathcal{A}_{18}$. The stable set $W^s(E^*)$ issues from $\mathcal{F}$ as well. (b) The repellor $\mathcal{F}$, which seems a weekly chaotic ring, separates the basin of attraction of the cycle $\mathcal{A}_{18}$ and that of $\{P^*, Q^*\}$. (c) Transversal crossing between the stable (in violet) and unstable (in green) sets of the saddle $\mathcal{S}_{18}$. (d) After the closure of the tangle involving the saddle of period 18, the stable branch ω^1_{18} comes from the repellor $\mathcal{F}$ and the unstable branch α^2_{18} converges to the focus cycle $\mathcal{A}_{18}$, giving rise to a saddle-focus connection. (e) An attracting closed curve exists in the phase-space, given by the saddle-focus connection.

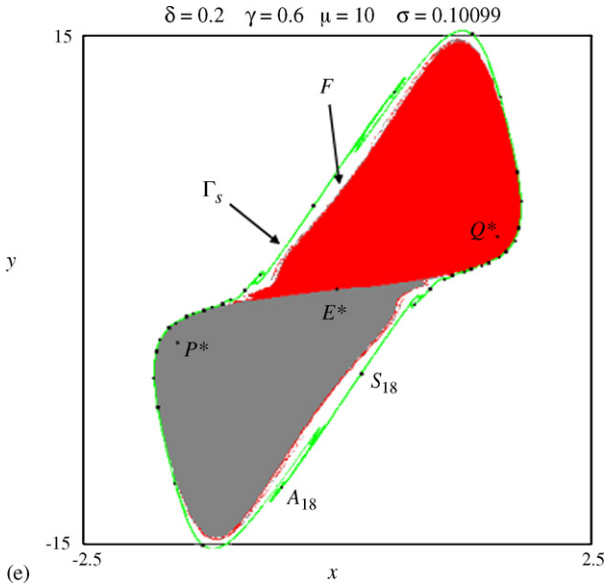

Fig. 5. (*Continued*).

lead us to conjecture a *saddle-node* bifurcation of closed invariant curves, we can certainly exclude this mechanism in the foregoing numerical example. Indeed the *saddle-node* bifurcation of a closed invariant curve is a known mechanism arising in continuous models, but very rare and *non-generic* in discrete maps. Global bifurcations similar to the ones illustrated in this section are responsible for the appearance of an attracting curve also in different regimes of the parameters, and similar mechanisms are likely to be at work also for low values of μ (as in the example presented in Fig. 2c), though in this case the parameter range in which the bifurcations take place may be very narrow. Note also that the global bifurcation sequence that we have described in this section is a mechanism similar to the one described in Agliari et al. (2005b), where the emergence of closed invariant curves is related to saddle connections. In our example, the mechanism is more complex with respect to the case analyzed in Agliari et al. (2005b), in that it involves at least two cycles and different homoclinic tangles.

4.2. *On the appearance of two repelling closed curves*

We proceed along the bifurcation path in order to study the mechanism which gives rise to the splitting of the repelling set $\mathcal{F}$. As the parameter σ is further increased an attracting closed curve Γ_s appears, substituting for the saddle-focus connection previously established. We have checked that the appearance of Γ_s is due to a global bifurcation, similar to that described in Agliari et al. (2005b) and still involving a heteroclinic tangle of the saddle $\mathcal{S}_{18}$, which destroys the saddle-focus connection. At its appearance Γ_s coexists with the cycles $\mathcal{A}_{18}$ and $\mathcal{S}_{18}$, surrounding them. Then the cycle $\mathcal{A}_{18}$ turns into a node, and a saddle-node bifurcation causes the disappearance of the two cycles. After the saddle-node bifurcation, Γ_s coexists with the two stable foci P^* and Q^*, as shown in Fig. 6a. The repellor $\mathcal{F}$ separates the basin of attractions of Γ_s and $\mathcal{A}$, the attracting set given by the union of the two stable foci. The basins of attraction of P^* and Q^* are separated by

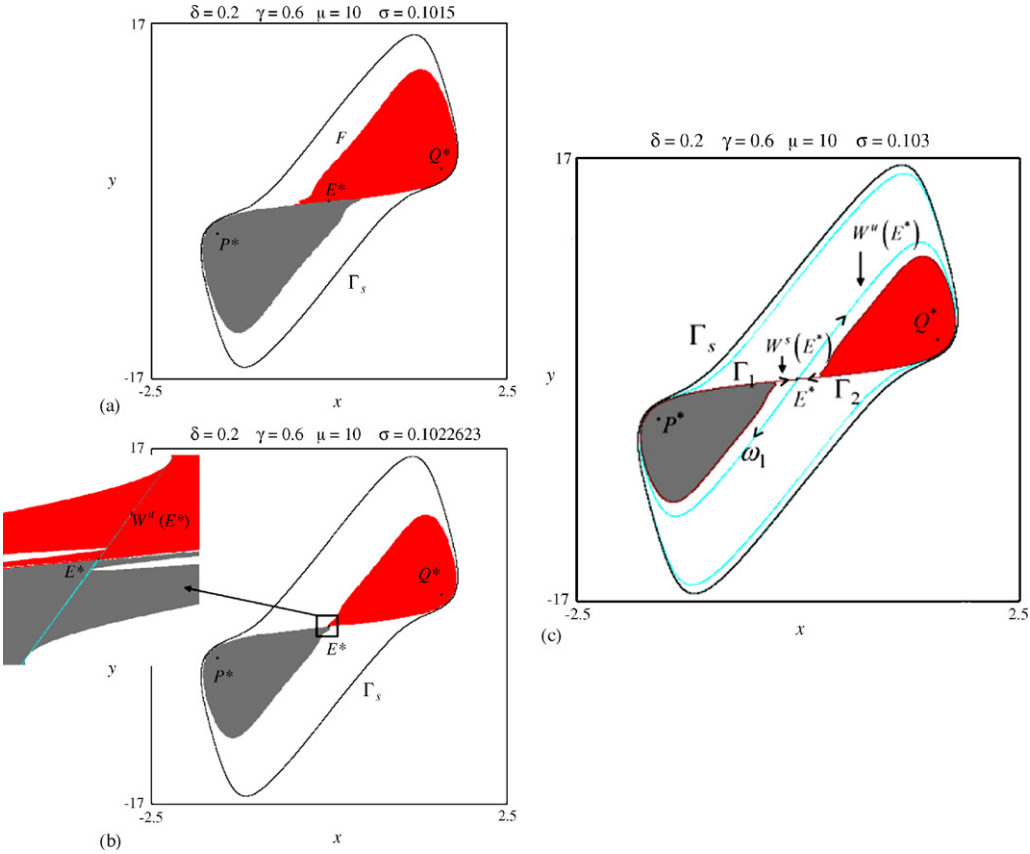

Fig. 6. Homoclinic bifurcation of E^*. (a) An attracting closed curve coexists with the two equilibria P^* and Q^*. A closed curve $\mathcal{F}$ bounds the set of self-sustaining trajectories. The trajectories converging either to P^* or Q^* are separated by the stable set $W^s(E^*)$. (b) At an intermediate value of σ, a tangency occurs between the stable and unstable sets of E^*, clearly observable in the enlargement. (c) At a larger value of σ, two repelling closed curves exist, each one bounding the basin of attraction of a fixed point. This is the first step of the homoclinic tangle which causes the disappearance of $\mathcal{F}$ and the appearance of the two repelling closed curves.

the stable set of the saddle E^*, which comes from $\mathcal{F}$. A branch α^1 of the unstable set of E^* reaches P^*, whereas the other one, α^2, reaches Q^*.

Continuing to increase the parameter σ, the set $\mathcal{F}$ shrinks to near the origin, showing more and more oscillations: this means that a homoclinic bifurcation of the saddle E^* is going to occur. In the enlargement of Fig. 6b the first homoclinic tangency between W^s (E^*) and W^u (E^*) is illustrated, after which the homoclinic tangle develops. After the second homoclinic tangency, as shown in Fig. 6c, the set $\mathcal{F}$ is split into two repelling closed curves (or some more complex chaotic repellors) Γ_1 and Γ_2, from which the branches ω^1 and ω^2, respectively, of the stable set of E^* issue. Also the unstable set of E^* has changed its behavior, converging to the attracting curve Γ_s.

The complete development of the homoclinic bifurcation of E^* is represented in Fig. 7, where the whole stable and unstable sets of E^* are drawn. The first homoclinic tangency is illustrated in Fig. 7a, obtained at the same parameters value as in Fig. 6b; the branch α^1 of W^u (E^*) converges to P^*, and it is completely contained in its basin of attraction; the same is true for α^2 with respect

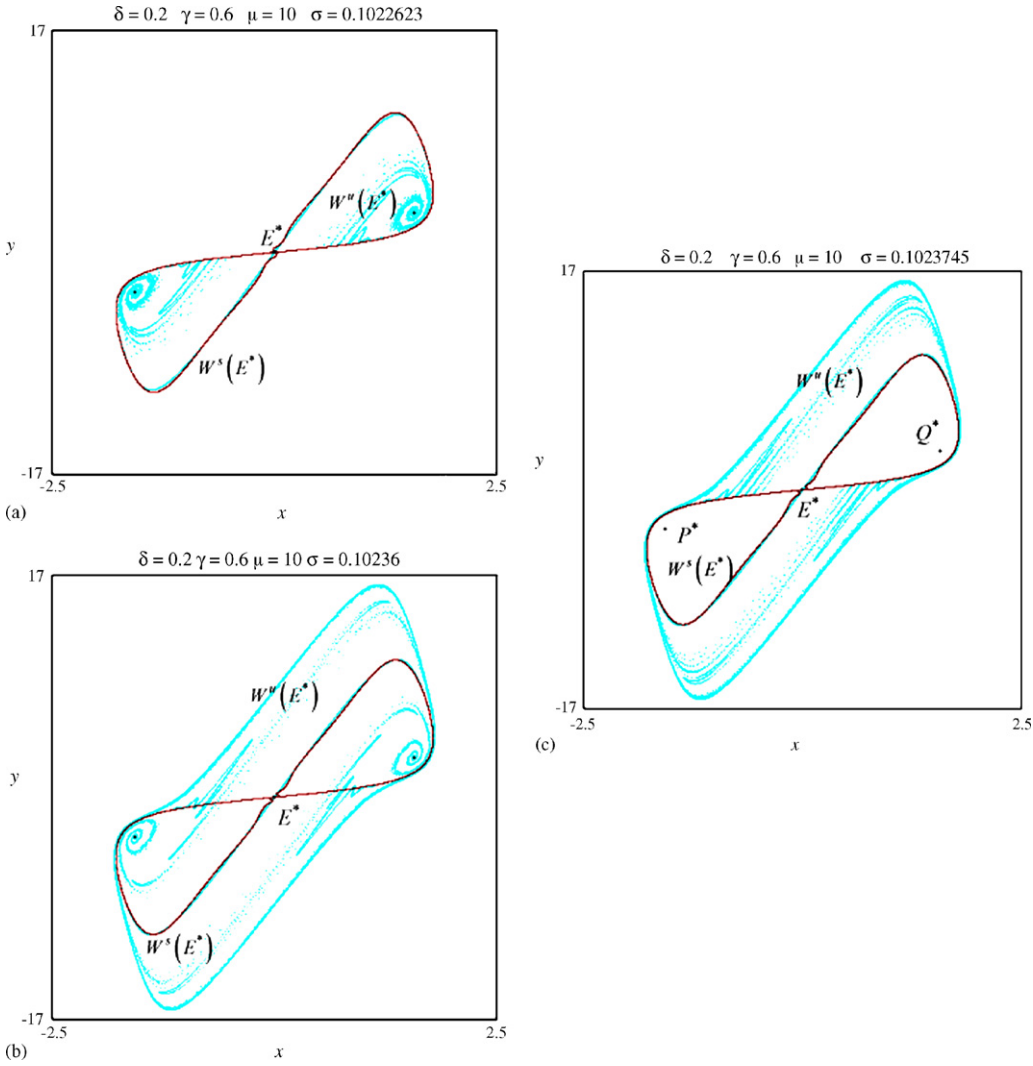

Fig. 7. The homoclinic tangle develops. (a) The first homoclinic tangency of $W^s(E^*)$ and $W^u(E^*)$, which opens the tangle. (b) The transversal crossing. (c) The second homoclinic tangency, at opposite side with respect to the previous one, which closes the homoclinic tangle.

to the fixed point Q^*. The stable branches have a complex structure; the repelling set $\mathcal{F}$ is replaced by a strange repellor, generated by the tangency and separating the basins of P^*, Q^* and Γ_s. The transversal crossing of W^s (E^*) and W^u (E^*) is shown in Fig. 7b. More and more homoclinic points of E^* are created; the separator of the three basins of attraction is a chaotic repellor, associated with the infinitely many periodic points existing close to the homoclinic trajectories. Moreover, we can observe that the unstable set W^u (E^*) enters the basin of attraction of the attracting closed curve Γ_s as well as that of the attracting set $\mathcal{A}$. As σ is further increased, more and more points of W^u (E^*) converge to Γ_s, and when the second homoclinic tangency occurs, no points of the unstable set converge to the two stable foci, as shown in Fig. 7c. This closes the tangle; the homoclinic

points of E^* disappear as well as the chaotic repellor, leaving the two disjoint curves Γ_1 and Γ_2 as boundaries of the basins of attraction of P^* and Q^*. After the homoclinic tangle both the branches of W^u (E^*) converge to the attracting closed curve Γ_s, and those of the stable set W^s (E^*) come from the repelling closed curves Γ_1 and Γ_2.

In the numerical example that has been chosen to explain the bifurcation sequences presented in the last two sections, we have assumed a high value of μ (adjustment parameter), because this allows us to "magnify" the mechanisms of transition between different scenarios. Indeed, based on numerical observations, we conjecture that similar mechanisms drive these bifurcation sequences in the generic case, in particular in cases of lower and more realistic values of μ. For instance the qualitative changes illustrated in Fig. 2 must involve some homoclinic (or heteroclinic) tangles, perhaps associated with saddle cycles of very high period. However, the parameter ranges in which these tangles develop may be very narrow ones, and it may be quite hard to detect them numerically and to illustrate the bifurcation sequence in detail.

The foregoing global analysis has explained some mechanisms which determine the *transition* between qualitatively different *dynamic scenarios characterized by coexistence of attractors*. The proposed example has shown that homoclinic bifurcations play an important role in such phase-space transitions. Moreover, transitions are of necessity associated with intermediate regimes, where homoclinic tangles are at work, in which chaotic repellors exist and the structure of the basins of the coexisting attractors may be quite complex. The economic relevance of these observations consists in the possibility of characterizing the typical bifurcation mechanisms that are associated with situations of coexisting attractors and, conversely, understanding which global changes (of attractors and basins of attraction) are likely to be observed when a specific bifurcation sequence is started. This could provide a guideline on the *global* dynamic analysis of economic models.

5. Conclusions

In this paper we have considered a particular version of the Kaldor business cycle model in discrete-time, which has been proposed in Bischi et al. (2001). The focus of the paper has been on the global bifurcations of attracting and repelling invariant curves which are associated with phenomena of coexistence of attractors and intricated structures of the basins of attraction, and this has been illustrated within the well known nonlinear framework of the Kaldor model. Our choice of the Kaldor model is due to the necessity of referring to a well understood nonlinear dynamic set-up, endowed with a rich (local) bifurcation structure which is able to generate qualitatively different dynamic scenarios (coexistence of two stable equilibria or long run fluctuations) in different regions of the space of parameters. This raises the important question (which has been considered in Bischi et al., 2001 at a rather intuitive level) of understanding the bifurcation mechanisms which produce the transition between different dynamic scenarios. We have shown that these bifurcation sequences involve homoclinic (or heteroclinic) tangles, associated with saddle points or saddle cycles of different period, and that the "intermediate" scenarios are of necessity accompanied by *complex structures of the basins of attraction*. This strengthens the role of *homoclinic bifurcation theory* (which has been recently introduced in economics in order to explain the *routes of complex attractors* which are often observed in numerical experiments) as a tool of analysis of *global dynamic phenomena*.

A final remark is about the economic implication of the global bifurcations illustrated in this paper. The question of equilibrium selection arises naturally within economic models charac-

terized by multiple equilibria. More generally (as is the case of the present model) under time evolution the system will select among multiple long-run dynamic outcomes which may include steady states and other types of attractors. In such cases, the graphical representation of the basins of attraction appears to be the only way to predict which attractor will be selected by the economy. However, numerical and graphical analysis may not be sufficient when a high degree of uncertainty in the selection of the final outcome is induced by the possibility that the basins of attraction are very intermingled, which may occur during the phase of a homoclinic tangle. For instance, in the case of Fig. 4a, *even in the presence of attractors with a relatively simple structure*, the final outcome of the system may be totally uncertain when the initial condition is selected in particular regions of the phase-plane, where the basin boundaries are very complicated sets with a fractal structure. This particular *notion of complexity*, which has received relatively little attention in the economic literature, refers to the "*final state" unpredictability* (see McDonald et al., 1985; Brock and Hommes, 1997) rather than to the erratic nature of the motion on a strange attractor. Nevertheless, the numerical and graphical approach that we have adopted, based on a thorough study of the qualitative changes of stable and unstable manifolds of saddles, might prove to be useful to discover those particular ranges of the parameters where transversal intersections and homoclinic tangles are developing, and where therefore one could expect dynamic phenomena similar to the ones studied in this paper.

Acknowledgments

This work has been performed as one of the activities of the national research project "Nonlinear Models in Economics and Finance: Complex Dynamics, Disequilibrium, Strategic Interaction", MIUR, Italy and in the framework of the Joint Research Grant (0382) "Reconsideration of economic dynamics from a new perspective of nonlinear theory", Chuo University, Tokyo, Japan. The authors wish to thank an anonymous referee and the editors of this special issue for valuable suggestions, which have led to a substantial improvement of this paper. The usual caveat applies.

Appendix A. Supplementary data

Supplementary data associated with this article can be found, in the online version, at doi:10.1016/j.jebo.2005.07.009.

References

Agliari, A., Dieci, R., 2005. Coexistence of attractors and homoclinic loops in a Kaldor-like business cycle model. In: Puu, T., Sushko, I. (Eds.), Business Cycle Dynamics—Models and Tools. Springer-Verlag, New York, pp. 223–254.

Agliari, A., Bischi, G.I., Dieci, R., Gardini, L., 2005a. Global bifurcations of closed invariant curves in two-dimensional maps: a computer assisted study. International Journal of Bifurcation and Chaos 15, 1285–1328.

Agliari, A., Gardini, L., Puu, T., 2005b. Some global bifurcations related to the appearance of closed invariant curves. Mathematics and Computers in Simulation 68, 201–219.

Agliari, A., Chiarella, C., Gardini, L., 2006. A re-evaluation of the adaptive expectations in light of global nonlinear dynamic analysis. Journal of Economic Behavior and Organization 60, 526–552.

Agliari, A., Gardini, L., Delli Gatti, D., Gallegati, M., 2000. Global dynamics in a nonlinear model for the equity ratio. Chaos Solitons Fractals 11, 961–985.

Bischi, G.I., Dawid, H., Kopel, M., 2003. Spillover effects and the evolution of firm clusters. Journal of Economic Behavior and Organization 50, 47–75.

Bischi, G.I., Dieci, R., Rodano, G., Saltari, E., 2001. Multiple attractors and global bifurcations in a Kaldor-type business cycle model. Journal of Evolutionary Economics 11, 527–554.

Bischi, G.I., Kopel, M., 2001. Equilibrium selection in a nonlinear duopoly game with adaptive expectations. Journal of Economic Behavior and Organization 46, 73–100.

Bischi, G.I., Kopel, M., 2003. Long run evolution, path dependence and global properties of dynamic games: a tutorial. Cubo A Mathematical Journal 5, 437–468.

Brock, W.A., Hommes, C.H., 1997. A rational route to randomness. Econometrica 65, 1059–1095.

Chang, W.W., Smyth, D.J., 1971. The existence and persistence of cycles in a non-linear model: Kaldor's 1940 model re-examined. Review of Economic Studies 38, 37–44.

Chiarella, C., Dieci, R., Gardini, L., 2002. Speculative behaviour and complex asset price dynamics: a global analysis. Journal of Economic Behavior and Organization 49, 173–197.

Dana, R.A., Malgrange, P., 1984. The dynamics of a discrete version of a growth cycle model. In: Ancot, J.P. (Ed.), Analyzing the Structure of Economic Models. Martinus Nijhoff, The Hague, pp. 205–222.

Dieci, R., Bischi, G.I., Gardini, L., 2001. Multistability and role of noninvertibility in a discrete-time business cycle model. Central European Journal of Operation Research 9, 71–96.

Dohtani, A., Misawa, T., Inaba, T., Yokoo, M., Owase, T., 1996. Chaos, complex transients and noise: illustration with a Kaldor model. Chaos Solitons Fractals 7, 2157–2174.

Droste, E., Hommes, C.H., Tuinstra, J., 2002. Endogenous fluctuations under evolutionary pressure in Cournot competition. Games and Economic Behavior 40, 232–269.

Foroni, I., Gardini, L., 2003. Homoclinic bifurcations in heterogeneous market models. Chaos Solitons Fractals 15, 743–760.

Foroni, I., Gardini, L., Rosser Jr., J.B., 2003. Adaptive and statistical expectations in a renewable resource market. Mathematics and Computers in Simulation 63, 541–567.

Gabisch, G., Lorenz, H.W., 1989. Business Cycle Theory, second ed. Springer-Verlag, Berlin.

Grasman, J., Wentzel, J.J., 1994. Co-existence of a limit cycle and an equilibrium in a Kaldor's business cycle model and its consequences. Journal of Economic Behavior and Organization 24, 369–377.

Guckenheimer, J., Holmes, P., 1983. Nonlinear Oscillations, Dynamical Systems, and Bifurcations of Vector Fields. Springer-Verlag, New York.

Gumowski, I., Mira, C., 1980. Dynamique Chaotique. Cepadues (Ed.), Toulouse.

Herrmann, R., 1985. Stability and Chaos in a Kaldor-Type Model. Working paper DP22, Department of Economics, University of Göttingen.

Kaldor, N., 1940. A model of the trade cycle. Economic Journal 50, 78–92 (reprinted in Essays on Economic Stability and Growth, 1964. Duckworth, London, pp. 177–192).

Kaldor, N., 1971. A comment. Review of Economic Studies 38, 45–46.

Kuznetsov, Y.A., 2003. Elements of Applied Bifurcation Theory, third ed. Springer-Verlag, New York.

Lorenz, H.W., 1987. Strange attractors in a multisector business cycle model. Journal of Economic Behavior and Organization 8, 397–411.

Lorenz, H.W., 1992. Multiple attractors, complex basin boundaries, and transient motion in deterministic economic systems. In: Feichtinger, G. (Ed.), Dynamic Economic Models and Optimal Control. North-Holland, Amsterdam, pp. 411–430.

Lorenz, H.W., 1993. Nonlinear Dynamical Economics and Chaotic Motion, second ed. Springer-Verlag, New York.

McDonald, S., Grebogi, C., Ott, E., Yorke, J., 1985. Fractal basin boundaries. Physica D 17, 125–153.

Medio, A., Lines, M., 2001. Nonlinear Dynamics. Cambridge University Press, Cambridge.

Mira, C., Gardini, L., Barugola, A., Cathala, J.C., 1996. Chaotic Dynamics in Two-Dimensional Noninvertible Maps. World Scientific, Singapore.

Pintus, P., Sands, D., de Vilder, R., 2000. On the transition from local regular to global irregular fluctuations. Journal of Economic Dynamics and Control 24, 247–272.

Palis, J., Takens, F., 1994. Hyperbolicity and Sensitive Chaotic Dynamics at Homoclinic Bifurcations. Cambridge University Press, Cambridge.

Puu, T., Sushko, I. (Eds.), 2002. Oligopoly Dynamics: Models and Tools. Springer-Verlag, New York.

Rodano, G., 1997. Lezioni sulle teorie della crescita e sulle teorie del ciclo, Working paper Dipartimento di Teoria Economica e Metodi Quantitativi, Universitá di Roma "La Sapienza".

Varian, H.R., 1979. Catastrophe theory and the business cycle. Economic Inquiry 17, 14–28.

de Vilder, R., 1996. Complicated endogenous business cycles under gross substitutability. Journal of Economic Theory 71, 416–442.

Appendix

In this Appendix we derive the region of invertibility of the map T in the space of parameters (i.e. we determine the combinations of parameters under which the "backward iteration" of (5) is uniquely defined), so that each point of the phase-space has a unique preimage of *rank-1*. Moreover, for those ranges of parameters where the map is noninvertible, we discuss the question of the number and the location of the preimages of a point of the phase space.

The rank-1 preimages of a point (u, v) are the solutions of the system

$$\begin{cases} u = (1-\gamma-\delta)\, x + \arctan y \\ v = -\mu\gamma x + (1-\mu\sigma)\, y + \mu \arctan y \end{cases}$$

where the unknown variables are x and y. Rearranging the two equations we obtain

$$\begin{cases} x = \frac{(1-\sigma\mu)y - v + \mu u}{\mu(1-\delta)} \\ -(1-\delta-\gamma)\frac{1-\sigma\mu}{\mu(1-\delta)} y + \frac{(1-\delta-\gamma)v + \gamma\mu u}{\mu(1-\delta)} = \arctan y \end{cases} .$$

Then the y-coordinate of the rank-1 preimages of the points (u, v) must satisfy the equation

$$q\,(u, v) + my = \arctan y \tag{12}$$

where $q\,(u, v) = \frac{(1-\delta-\gamma)v + \gamma\mu u}{\mu(1-\delta)}$ and $m = (\gamma+\delta-1)\frac{1-\sigma\mu}{\mu(1-\delta)}$.

Simple geometrical considerations allow us to check that if $m < 0$ or $m \geq 1$, equation (12) has a unique solution for any given (u, v). Therefore if

$$(\gamma+\delta-1)\,(1-\sigma\mu) < 0 \quad \text{or} \quad (\gamma+\delta-1)\,\frac{1-\sigma\mu}{\mu\,(1-\delta)} \geq 1$$

the map T is invertible (i.e. it has a unique inverse). If $m = 0$, then a unique solution of (12) exists if $-\pi/2 < q\,(u, v) < \pi/2$; otherwise no solution exists.

In the case $0 < m < 1$, one, two or three solutions of the equation (12) may exist depending on the value of $q = q\,(u, v)$. In particular, for a given m, $0 < m < 1$, two solutions exist if the straight line at the left side of (12) is tangent to the S-shaped curve $f\,(y) = \arctan y$; that is if

$$m = \frac{1}{1+y^2}$$

so that $y = \mp\sqrt{\frac{1}{m} - 1}$, and

$$\begin{aligned} q\,(u, v) &= q_1 = m\sqrt{\frac{1}{m} - 1} - \arctan\sqrt{\frac{1}{m} - 1} \\ q\,(u, v) &= q_2 = -m\sqrt{\frac{1}{m} - 1} + \arctan\sqrt{\frac{1}{m} - 1} \end{aligned}$$

with $q_1 < q_2$.

Moreover, if $q\,(u, v) < q_1$ or $q\,(u, v) > q_2$ the equation (12) has a unique solution (and the point (u, v) has a unique preimage) while if $q_1 < q\,(u, v) < q_2$ three solutions exist (and therefore three different preimages of the point (u, v)).

This means that if

$$\begin{cases} (1-\delta-\gamma)\,(1-\sigma\mu) < 0 \\ (1-\delta-\gamma)\frac{1-\sigma\mu}{\mu(1-\delta)} > -1 \end{cases} , \tag{13}$$

the map T is noninvertible and, following the notation used in Mira *et al.*, it is a so-called $Z_1 - Z_3 - Z_1$ *map*. With such a notation we indicate that the phase plane is divided in different regions Z_1 and Z_3, whose points have one and three different rank-1 preimages, respectively. Such regions, or *zones*, are separated by the *critical line* LC (i.e. the locus of points having two merging rank-1 preimages).

It follows from the above considerations that the critical line LC is the locus of the points (x, y) of the phase-plane which satisfies[1]

$$q(x, y) = q_1 \quad \text{or} \quad q(x, y) = q_2,$$

and therefore LC is made up by two distinct branches; that is $LC = L^a \cup L^b$ with

$$\begin{aligned} L^a \quad &: \quad x = \frac{(\delta + \gamma - 1)}{\gamma\mu} y + \frac{(1 - \delta)}{\gamma} q_1 \quad \text{and} \\ L^b \quad &: \quad x = \frac{(\delta + \gamma - 1)}{\gamma\mu} y + \frac{(1 - \delta)}{\gamma} q_2 \ . \end{aligned} \tag{14}$$

The locus of the merging preimages of the points belonging to the set LC is the rank-0 critical line LC_{-1} and it is given by $L^a_{-1} \cup L^b_{-1}$, where

$$\begin{aligned} L^a_{-1} \quad &: \quad y = -\sqrt{\frac{1}{m} - 1} \\ L^b_{-1} \quad &: \quad y = \sqrt{\frac{1}{m} - 1} \end{aligned} \tag{15}$$

(i.e. the points which satisfy the tangency condition).

From the noninvertibility conditions (13) we obtain that, for $\delta + \gamma < 1$, the noninvertibility region is an unbounded subset of the (μ, σ)-plane defined by

$$\sigma > \frac{1}{\mu}$$

given that the second condition of (13) is always fulfilled for $0 < \sigma < 1$; for $\delta + \gamma > 1$, the noninvertibility region is defined by

$$\frac{1}{\mu} - \frac{1 - \delta}{\gamma + \delta - 1} < \sigma < \frac{1}{\mu} \ .$$

[1] We recall that the critical line of the map T in (5) may also be obtained by $LC = T\,(LC_{-1})$, where LC_{-1} is the locus of points at which the determinant of the Jacobian matrix vanishes, given in the following equation (15).